ELSEVIER

Polymer 41 (2000) 3993–4004

polymer

Fundamental studies of a novel, biodegradable PEG-*b*-PLA hydrogel

A.T. Metters, K.S. Anseth*, C.N. Bowman

Department of Chemical Engineering, University of Colorado at Boulder, Boulder, CO 80309-0424, USA

Received 18 May 1999; accepted 28 July 1999

Abstract

The degradation behavior of highly swollen, chemically cross-linked hydrogels was characterized by monitoring changes in their mass loss, degree of swelling and compressive modulus. The hydrogels were used as model systems to investigate the hydrolytic degradation process in cross-linked networks. The trends of the three measured properties differ substantially from those seen for linear degradable systems; however, they can still be predicted accurately using hydrolysis kinetics and network structure. Experimental results show that the modulus decreases exponentially with time while the volumetric swelling ratios for these gels increase exponentially. The characteristic exponential time constants for these two functions, as well as the overall degradation timescale, are influenced greatly by the network structure. Thermodynamic relationships are used to explain these trends as well as relating the observed tradeoff between the two desirable properties of mechanical strength and water content.

Keywords: Hydrogel; Biodegradable; Cross-linking density

1. Introduction

Biodegradable, hydrophobic polymers such as poly(lactic acid) (PLA) and poly(glycolic acid) (PGA) have been used for many years as sutures, staples, and for the controlled release of certain drugs [1–3]. Although widely investigated because of their biocompatibility and bioresorbability, the applications of these hydrolytically bulk-degrading polymers are limited by several factors. For example, difficulty in homogeneous dispersal of hydrophilic materials within such hydrophobic polymer matrices leads to inconsistent drug release profiles. There exists a need for materials that do not stimulate an inflammatory response by the host and can be used for sustained release of hydrophilic bioactive macromolecules such as therapeutic proteins, peptides, and oligonucleotides.

Hydrogels made from cross-linked poly(ethylene glycol) (PEG) have emerged as a potential solution to the problems created by hydrophobic polymer matrices. Because they are highly hydrated, non-ionic, and relatively resistant to protein adsorption and cell deposition, PEG hydrogels have attracted the attention of researchers for a variety of practical applications that could not be served by hydrophobic polymers such as PLA. The prolonged release of several bioactive drugs from these materials has been reported [4–6]. The high degree of swelling observed in these hydrogel networks, however, greatly limits their mechanical strength. In addition, PEG is non-degradable on any useful timescale, necessitating physical removal of any implanted device.

Copolymerization of PEG with lactides has overcome the drawbacks of hydrophilic hydrogels while taking advantage of the proven usefulness of hydrophobic, biodegradable polymers. Separately, both PEG and PLA present shortcomings, as mentioned above. Together, however, copolymerization constitutes an attractive means of modulating the basic properties of each homopolymer. Through variation of the hydrophilic/hydrophobic segment ratios, copolymerization of PEG with PLA is now regarded as a means to obtain new polymeric materials with novel physical, chemical, and biological properties adaptable to specific uses [7–9].

The PEG/PLA copolymerization scheme was improved further through development of hydrophilic, degradable polymer networks. Sawhney et al. [9] described the synthesis of a triblock PEG-*b*-PLA copolymer with acrylate end groups (see Fig. 1). Each domain along the macromer plays a specific role in the resulting hydrogel function: the PEG backbone gives the hydrogel its hydrophilicity, the hydrolytically labile PLA linkages provide biodegradability, and the polymerizable end groups provide the means to form a cross-linked network. The ratio of PEG to PLA segments can be used to manipulate a number of physical properties from the permeability of the gel to its degradation rate [9,10]. Hubbell and others have proven the usefulness of

* Corresponding author. Tel.: +1-303-492-3147; fax: +1-303-492-4341.
E-mail address: kristi.anseth@colorado.edu (K.S. Anseth).

0032-3861/00/$ - see front matter
PII: S0032-3861(99)00629-1

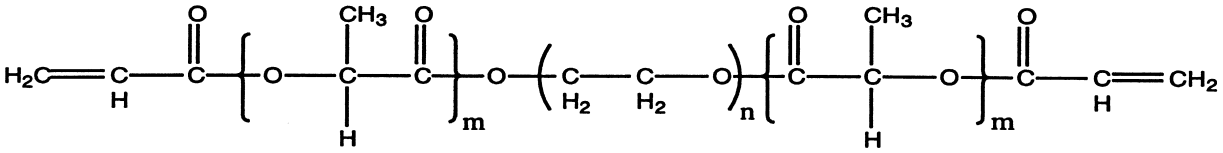

Fig. 1. Schematic of the biodegradable, PEG-*b*-PLA macromer.

these gels in a number of biomedical applications: (1) as a barrier material to prevent postsurgical adhesion formation in animal models [11]; (2) to prevent thrombosis and vessel narrowing following vascular injuries [12]; and (3) as vehicles for controlled in vitro release of various proteins and oligonucleotides [10]. These networks have also shown great promise as temporary scaffolds to enhance the regrowth of a number of important tissues such as cartilage and bone [13].

The degradation behavior of the novel PEG-*b*-PLA hydrogels plays a key role in determining the success or failure of these materials for each application. Although the chemical reactions by which these gels degrade are known, the macroscopic behavior they exhibit during degradation is not well understood. Drug-release and degradation rates are known to be affected by such chemical parameters as comonomer ratio and polymer molecular weight [9,10,14]. Still unknown, however, is the influence of the network microstructure upon such properties. It is well documented that the physical and mechanical behaviors of a hydrogel are highly dependent on its backbone chemistry and cross-linking density [15]. It is, therefore, clear that the degradation behavior of the gel will be a function of its network topology as well.

The objective of this research is to monitor the degradation behavior of the novel PEG-*b*-PLA hydrogels through mass, swelling, and mechanical strength measurements. The impact of the network microstructure and comonomer chemistry on the macroscopic, physical properties of these gels during degradation is also quantified. The degradation behavior differs greatly from that seen in linear systems studied previously. These hydrogels are used as model systems to investigate the hydrolytic degradation process in cross-linked, hydrophilic networks. The added ability to adjust network structure by controlling the degree of cross-linking within the gel should also increase the versatility and efficacy of degradable hydrogels in a wide variety of biomedical applications.

2. Materials and methods

The multifunctional macromer used in this study (see Fig. 1) was synthesized according to the techniques and procedure first described by Sawhney et al. [9]. The notation given for the macromer refers to the molecular weight of the PEG chain followed by the symmetrical number of lactide repeating units on each end. For example, 4600-5, the macromer used for all experiments, refers to a macromer containing a 4600 molecular weight PEG chain with an average of five repeating lactide units on either side. Both ends of this copolymer chain are then end-capped with acrylate functionalities to allow photopolymerization and cross-linking of the chains. The polymers and reagents used for the synthesis of the macromer included: 4600 PEG (Aldrich), DL-lactide (Polysciences), triethylamine (Aldrich), acryloyl chloride (Aldrich), diethyl ether (Fisher), and stannous octoate (Aldrich). All chemicals were used as received.

Photopolymerization of the macromers was carried out under a visible light source (Electro-Light Corporation) with a peak intensity of 15 mW/cm^2 at a wavelength of 420 nm to produce hydrogels of varying composition and structure. The solid 4600-5 macromer was dissolved in deionized water to a given concentration (25, 50, or 70 wt%). For some of the data sets, a specified amount of acrylic acid (Aldrich) was mixed with the macromer. A 10 wt% solution of Quantacure ITX photosensitizer (Biddle Sawyer Corporation) and Irgacure 907 (I-907) initiator (Ciba Geigy) dissolved in ethanol was then added to the final macromer solution until the total I-907 concentration was 0.10 wt%. For the polymerization studies, reaction rate profiles were monitored with a differential scanning calorimeter (DSC-DPA 7; Perkin–Elmer). For degradation studies, the solution was placed between two glass slides approximately 1.0 mm apart and polymerized into solid disks. Each side of the disk was exposed to the light source for approximately 10 min to ensure maximum conversion of the macromer.

Degradation of the polymerized hydrogel was carried out in a 7.4 pH phosphate-buffered saline solution (Fisher) at 37°C. The polymerized disks were each weighed (m), placed in a permeable, plastic tissue holder, and immersed in enough buffer solution to maintain the bulk pH at 7.4 throughout the entire degradation experiment (~30 ml). At specified time points (roughly three times per day), one to three disks were removed from the degradation medium; their swollen mass was measured in both air and heptane to obtain the swollen polymer volume; their static compressive modulus was then obtained using a dynamic mechanical analyzer (Perkin–Elmer) with a parallel plate configuration and a ramping stress of 400 mN/min; and their final mass (m_p) was obtained after complete drying in a vacuum oven. The initial dry polymer mass (m_{pi}) was calculated by combining the weight of the polymerized solution (m) and the weight fraction of macromer in that solution (x_i) in the

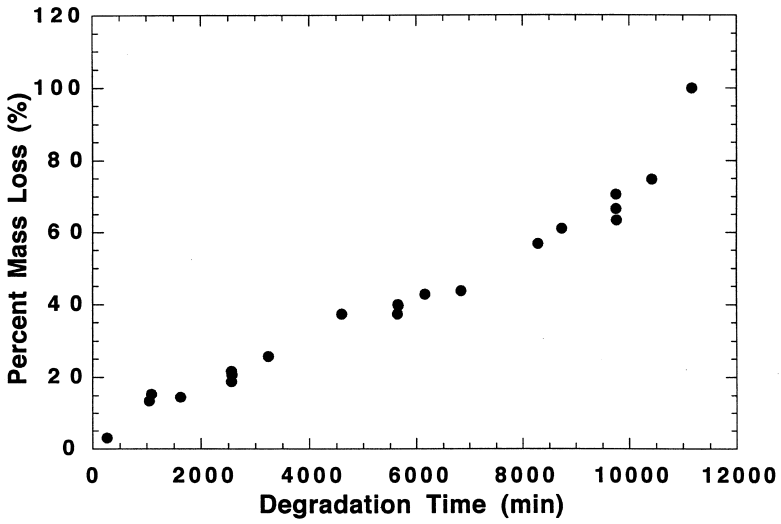

Fig. 2. Experimentally measured mass loss for a hydrogel polymerized from a 50 wt% solution of 4600-5 PEG-*b*-PLA macromer.

following manner:

$$m_{pi} = mx_i \quad (1)$$

The percent mass loss of each sample was then determined using the following equation:

$$\%\ \text{mass loss} = \frac{(m_{pi} - m_p)}{m_{pi}} 100\% \quad (2)$$

3. Results and discussion

3.1. General degradation behavior

Fig. 2 shows a typical mass loss curve for a degrading PEG-*b*-PLA copolymer hydrogel. The curve appears linear throughout most of the degradation, corresponding to an approximately constant mass-loss rate. During the last 20% of mass loss the rate of degradation increases sharply. This high mass-loss rate continues until none of the original cross-linked network remains.

The degradation behavior of linear PLA systems, in contrast, is much different from the behavior observed in Fig. 2 [16,17]. The mass loss of these linear systems is characterized by two distinct phases. During the first phase, no mass loss is observed although the molecular weight of the polymer chains decreases continuously. After this time lag, which varies with molecular weight, crystallinity, and polymer chemistry, mass loss spontaneously occurs at a very high rate. Following this sudden transition, the second characteristic phase begins. During this final step the mass-loss rate from the sample continuously decreases until none of the original, solid specimen remains. From the unusual shape of the hydrogel mass loss curve in Fig. 2, it is evident that the degradation of the cross-linked networks formed from the PEG-*b*-PLA macromers is a dynamic process very different from that of linear polymeric systems. The uniqueness of the curve in Fig. 2, as well as data which will be presented in the following sections, is due not only to the novel chemistry of the starting macromers and their hydrolysis kinetics, but, as will be shown, is also related to the structure of the cross-linked network they form.

As discussed in the introduction, the PEG-*b*-PLA macromers used to form the hydrogels under study in this paper are multifunctional with a double bond located on each end

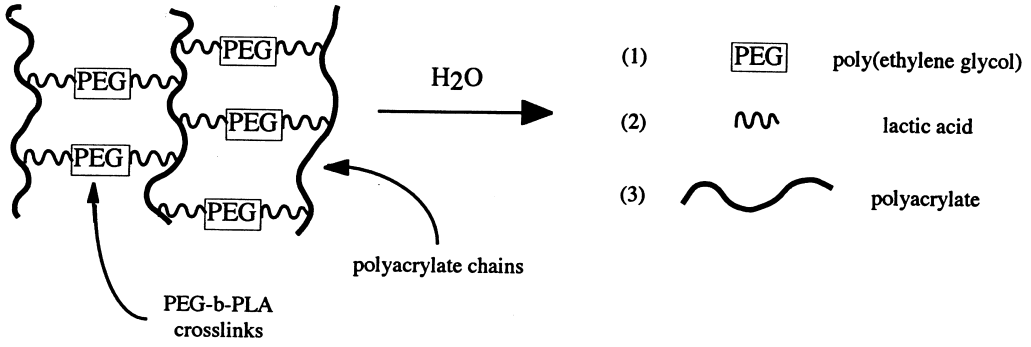

Fig. 3. Idealized cross-linked hydrogel structure from the PEG-*b*-PLA macromer, and its degradation products after hydrolysis of the PLA linkages.

of the macromer chain. A three-dimensional network is formed through the chain polymerization of these acrylate functional endgroups. The result of such a reaction is a model hydrogel consisting of two distinct building blocks: (1) polyacrylate chains formed through the polymerization reaction; and (2) PEG-*b*-PLA copolymer cross-links from the macromer backbone. The way in which these blocks form a continuous network is illustrated in Fig. 3. The cross-links, PEG-*b*-PLA chains, connect the kinetic polyacrylate chains. With only the acrylate groups forming the polymerized backbone of the network, the vast majority of the network mass resides in its PEG-*b*-PLA cross-links. In the 4600-5 macromer, for example, the PEG-*b*-PLA segments account for approximately 95% of the total macromer mass. From a thermodynamic perspective the cross-links are what bind the network together, preventing the individual kinetic chains from dissolving into the surrounding solution by providing a retractive force. This retractive force also provides the hydrogel with a mechanical elasticity or strength.

The PEG-*b*-PLA segments also contain the hydrolytically labile ester bonds that provide the network with its degradable characteristic. When exposed to water, these linkages within the PLA segments are cleaved at a rate given by the hydrolysis kinetics. The microscopic breaking of these specific bonds within the network leads to the mass loss observed in Fig. 2 and the macroscopic degradation of the hydrogel over time into the products shown in Fig. 3. Reaction kinetics can therefore be used to estimate the number of intact, water-labile PLA segments as a function of degradation time.

The kinetics of ester hydrolysis reactions for PLA are well studied. The reaction has been shown to be acid-catalyzed and dependent upon the concentration of acid catalyst, surrounding water, and the ester itself [18–20]. The acid species used to catalyze this reaction come from either hydronium ions found in the solvent solution or, as shown in Fig. 3, from the lactic acid and carboxylic acid end groups formed during degradation. Since the p*K*a of lactic acid and its oligomers is approximately three [21], the dissociation of the acid end groups can be a significant source of hydronium ions at neutral or basic pHs. This statement is especially true for pure PLA samples, which generally have low water contents because of their hydrophobicity. When such conditions exist, the promotion of the hydrolysis reaction by its acidic products leads to auto-catalytic behavior and dramatic increases in degradation rates as the reaction proceeds.

The hydrogels currently under study, however, are very different from pure PLA networks. Since they are copolymers with the PLA segments contributing only a fraction to the overall molecular weight, their acid group concentration is much lower. Also, because of the presence of the hydrophilic PEG blocks, these gels are much more highly swollen than pure PLA systems. This high degree of swelling lowers the concentration of all acidic species within the cross-linked networks and also allows more efficient removal of degradation products from the system. In addition, all of the experiments were conducted in a phosphate buffered solution, which remained at a constant pH of 7.4 during the entire degradation process. These characteristics indicated the ability of the solution to neutralize any acidic reaction products. With all of these factors pointing to the absence of auto-catalytic effects within the PEG-*b*-PLA hydrogels, the kinetic equation for their degradation can be written as:

$$\frac{d[E]}{dt} = -k[E][H_2O][H_3O^+] \tag{3}$$

where [E] is the ester concentration in the PLA segments, $[H_2O]$ is the water concentration within the swollen hydrogel, $[H_3O^+]$ is the concentration of hydronium ion in the buffer solution, t is degradation time, and k is the kinetic rate constant.

Eq. (3) can be simplified by combining constant terms. The highly swollen nature of these particular hydrogels allows the argument to be made that the water concentration remains relatively constant during degradation. In addition, it has already been reasoned that auto-catalytic effects do not play a significant role in the degradation of these gels. The acid-catalyst concentration will, therefore, also remain nearly constant during degradation. These assumptions lead to the following pseudo first order kinetic equation for the cleavage of the lactide bonds within these hydrogels:

$$\frac{d[E]}{dt} = -k'[E] \tag{4}$$

Here k' is the pseudo first order kinetic constant that is the product of the original kinetic constant k and the approximately constant water and acid concentrations. Integrating and solving for [E] in Eq. (4) leads to an exponentially decaying ester concentration versus time. Since two blocks of degradable ester groups reside along either side of the PEG-*b*-PLA cross-links as shown in Figs. 1 and 3, statistical relationships imply that the concentration of active cross-links within the system and the cross-linking density of the hydrogel decay exponentially in time as well. Many researchers have demonstrated the importance of cross-linking density on hydrogel performance [15], and, as will be shown in a later section, cross-linking density determines many of the macroscopic properties of the current hydrogel during degradation.

The hydrolysis kinetics predict not only a decrease in the concentration of water-labile ester groups ([E]) as degradation proceeds, but also a decrease in the rate at which these linkages are broken ($d[E]/dt$). Based on this kinetic information, treating the PEG-*b*-PLA cross-links as independent chains rather than as a connected network will lead to the prediction that the mass-loss rate will decrease with time as well. For linear systems of PLA and other degradable polymers this trend has been observed experimentally [16,22]. From the data in Fig. 2, however, this prediction is incorrect

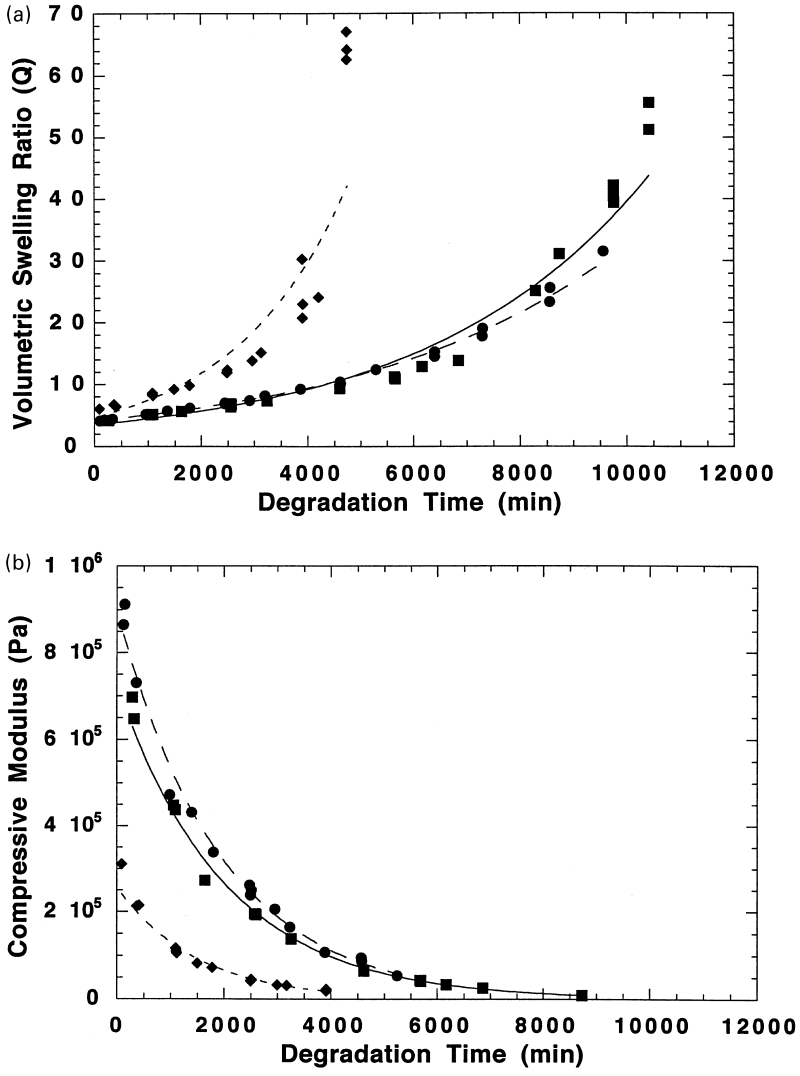

Fig. 4. Swelling (a) and compressive modulus (b) as a function of degradation time for hydrogels polymerized with varying macromer concentrations: (◆) 25 wt%; (■) 50 wt%; and (●) 70 wt%. The solid and dashed lines are exponential curves fit to the data points with time constants of 0.00046 min^{-1} (25 wt%), 0.00024 min^{-1} (50 wt%), and 0.00021 min^{-1} (70 wt%) for the swelling and $-0.00068\ min^{-1}$ (25 wt%), $-0.00050\ min^{-1}$ (50 wt%), and $-0.00044\ min^{-1}$ (70 wt%) for the modulus.

for the degradable systems in this study. Here, as mentioned previously, the polymers are structured into three-dimensional, cross-linked networks as opposed to linear polymer chains. The kinetic relationships for the hydrolysis and cleavage of the bonds along the polymer chains are still the same, but now the structure of the network also plays a role in determining the macroscopic degradation behavior of the hydrogel.

Taking into consideration the cross-linked structure of the hydrogels formed from the PEG-*b*-PLA macromers, the behavior of the mass-loss curve in Fig. 2 can be explained. As described in Section 1, the water-labile PLA segments of the macromer are present on either side of a relatively large PEG chain. As each PEG chain is linked to the rest of the polymerized network by only two degradable lactide oligomer blocks, this segment will be the first type released from the gel. The degradation of these broken cross-links and their diffusion out of the gel form the initial portion of the mass-loss curve.

Just as the rate of degradation of ester linkages decreases with degradation time, the release rate of individual cross-links will decrease with time as well. The rate of mass loss is held constant in Fig. 2, however, due to the additional release of polyacrylate chains from the network. Each polymerized chain of polyacrylate is held in place by numerous cross-links. Only when all of these cross-links have been broken will a polyacrylate chain finally be released from the rest of the gel. The probability of this occurring is very low at the start of the degradation process, but increases significantly as the fraction of degraded cross-links approaches 100%. The release of such chains, along with several attached PEG-*b*-PLA segments, with ester bonds only broken on one side, accelerates the rate of mass loss observed during the later stages of degradation. For the

system shown in Fig. 2, this increase in mass-loss rate is offset by the decrease due to slowing degradation kinetics, producing a nearly constant rate until approximately 80% total mass loss.

The final burst of mass loss can also be explained by the structure of the cross-linked hydrogel. As the lactide linkages are hydrolyzed and the cross-links are continually broken, a point is reached where the remaining polymer chains no longer combine to form a gel with an infinite weight-averaged molecular weight ($\bar{M}_W$). This event is essentially the opposite of the gel point conversion that occurs during the polymerization of multifunctional macromers. When enough cross-links have been broken, all that remains of the three-dimensional network are separate polymer chains. These highly branched, yet uncross-linked, chains are soluble in the buffer solution. Their dissolution into the surrounding media results in an almost instantaneous loss of the remaining network mass.

3.2. Effect of macromer concentration

In addition to monitoring the loss of mass from the hydrogels as a function of time, two macroscopic properties, mechanical strength and swelling, were followed to aid in understanding the changes occurring within the network during the degradation process. Degradation in these swollen systems is known to be a complex function of several variables. Simultaneous monitoring of the changes in mass, mechanical strength, and swelling during degradation allows several of the controlling factors behind the degradation process to be decoupled and examined individually.

First, the degradation behaviors of hydrogels polymerized in solution with three different concentrations of macromer (25, 50, and 70 wt%) were monitored. All other conditions during network formation and degradation were held constant. Increasing the amount of solvent present during a non-linear, radical polymerization lowers the double bond concentration in the bulk solution. The local concentration of pendant double bonds surrounding a radical, however, remains constant. Since the bulk concentration of double bonds is lowered, the radical cannot react away from its pendant as quickly and spends an increased amount of time in its vicinity. This increased exposure of the PEG-*b*-PLA pendant heightens its reactivity with the radical and, therefore, increases the chances of the pendant reacting to form a primary cycle rather than a cross-link [23]. Since there is a tradeoff between cycles and cross-links, increasing the degree of cyclization decreases the cross-linking density within the gelled network. Even with the same polymer chemistry, such a change in network structure can have a dramatic impact on the macroscopic degradation behavior of the hydrogels.

Increasing the solvent concentration during polymerization of these hydrogels has many direct influences on their network structure in addition to increased cyclization. From the theoretical kinetic equations for initiation, propagation, and termination, one quickly realizes that kinetic chain lengths will be altered to some extent, as will the initiation efficiency and the degree of autoacceleration during polymerization. Although the effect of each of these changes may be small, lumped together they act to form dramatically different network structures. These differences can be seen in the swelling and modulus results during the degradation of these gels.

In Fig. 4a the volumetric swelling ratios (Q) of the three hydrogel sets polymerized with various concentrations of macromer are plotted versus degradation time. As indicated by the best-fit exponential functions, the swelling of these hydrogels is observed to increase exponentially with degradation time. Initially, the degree of swelling shows only a slight increase as macromer concentration decreases. As degradation proceeds, however, the effect of macromer concentration increases. The sample with the lowest macromer concentration (25 wt%) experiences the fastest growth in its swelling ratio, and therefore, swelling values above those of the other two samples over the entire course of its degradation. The final stage of degradation and mass loss of these samples is indicated by the sharp upsweep in the swelling versus time curves. This response occurs at longer times for increasing macromer concentrations.

Qualitatively, the trend in the swelling data agrees with the kinetic degradation mechanism proposed in the previous section where the ester concentration and number of intact cross-links within the network decay exponentially. As cross-links within the network are broken, the average molecular weight between the cross-links ($\bar{M}_C$) will increase at an exponential rate dictated by the degradation kinetics. According to the Flory–Rehner equation, the equation most widely used for characterizing the swelling of hydrogels, the degree of swelling (Q) increases as $\bar{M}_C$ increases [24]. In agreement with this theory, the data in Fig. 4a shows the swelling of the hydrogels increasing exponentially versus degradation time.

From the Flory–Rehner relationship, a comparison between the individual swelling curves can also be made. If cyclization increases with solvent content during polymerization then, holding all other parameters constant, $\bar{M}_C$ should also increase with solvent content due to less effective cross-linking during the polymerization. The Flory–Rehner equation then states that the degree of swelling at equilibrium will increase as the macromer concentration during polymerization is lowered. Although hard to distinguish at early times, the initial swelling ratios in Fig. 4a follow this trend with the amount of equilibrium swelling at each time point increasing with decreasing macromer concentration.

Recall from the discussion of degradation kinetics that the exponential decay for the concentration of active cross-links held true when the swelling was assumed to remain approximately constant during degradation. From the data in Fig. 4a the volumetric swelling ratio is shown to change by an order of magnitude during the degradation of all three hydrogels.

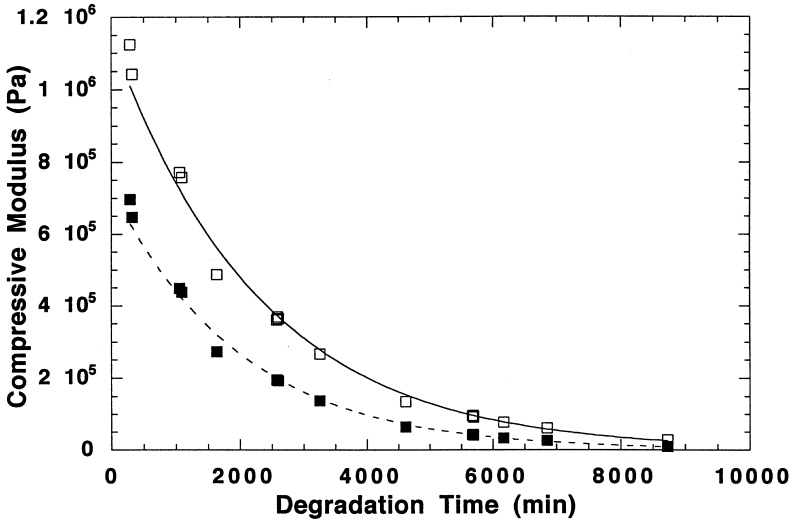

Fig. 5. The compressive modulus (■) and normalized compressive modulus (□) as a function of degradation time for a hydrogel polymerized from a 50 wt% solution of 4600-5 macromer. The time constants for the exponential-curve fits are $-0.00050\ \text{min}^{-1}$ (■) and $-0.00043\ \text{min}^{-1}$ (□).

This large shift in swelling may appear to be an enormous change, which should discount the earlier assumptions and make the exponential decay of cross-links an invalid conclusion. However, because of our high initial swelling ratios ($Q > 4$), the increase in the swelling of these gels over the course of their degradation reflect changes in water concentration of less than 20%. Therefore, the assumption of a constant water concentration during degradation and an exponential decay in the cross-linking density of these gels are still reasonably valid, and the qualitative conclusions we draw from these relationships are still accurate.

In Fig. 4b the compressive modulus of each sample is plotted versus its exposure time in the phosphate buffered solution. At $t = 0$, it can be seen that the initial modulus increases with macromer concentration. The sample polymerized with 70 wt% macromer attains compressive modulus values approaching 1 MPa. An important trend shared by all three curves is the exponential decrease in their modulus values with degradation time. The dashed lines through the data sets represent best-fit exponential decay functions. From these best-fit curves it is observed that the modulus decay rate decreases as macromer concentration increases. Both the slower decay rate and higher initial modulus values lead to longer degradation timescales as the macromer concentration is increased.

At first glance it is difficult to draw any straightforward conclusions between the compressive modulus data shown in Fig. 4b and the degradation behavior proposed in early sections. Two independent factors each contribute to the mechanical strength of a swollen hydrogel network: cross-linking density and polymer volume fraction. Cross-linking density, as already discussed, is inversely related to $\bar{M}_C$ and depends on the structure of the network. The polymer volume fraction ($\nu_{2,S}$), on the contrary, is inversely proportional to the degree of swelling (Q), another macroscopic property of the hydrogel (shown in Fig. 4a). Thus, the complexity of characterizing the relationship between the degradation behavior and the mechanical strength of these hydrogels becomes evident since the mechanical strength and degradation are both coupled to the swelling, and the swelling, as shown in Fig. 4a, is a function of the degradation.

Through rubber elasticity theory, contributions from both the structure of the hydrogel and its degree of swelling appear in the calculation of shear stress for a swollen system [25]:

$$\tau_S = \frac{\rho R T}{\bar{M}_C}(\nu_{2,S})^{1/3}\left(\frac{r_0^2}{r_f^2}\right)\left(1 - \frac{2\bar{M}_C}{\bar{M}_N}\right)\left(\lambda_S - \frac{1}{\lambda_S^2}\right) \tag{5}$$

In this equation, τ_S is the shear stress; ρ the density of the dry polymer; R the gas constant; T the temperature in Kelvin; (r_0^2/r_f^2) the front factor and is the ratio of end-to-end distance for network polymer chains versus isolated chains; $\bar{M}_N$ the number average molecular weight of the linear polymer chains before cross-linking; and λ_S the strain extension ratio. Approximating the front factor (r_0^2/r_f^2) as 1, neglecting chain ends ($\bar{M}_N \gg \bar{M}_C$), and inserting the relationship between compressive modulus (K) and shear modulus for an isotropic material gives the following equation:

$$K = \left(\frac{2(1+\nu)}{3(1-2\nu)}\right)\frac{\rho R T}{\bar{M}_C}(\nu_{2,S})^{1/3} \tag{6}$$

Here, ν is Poisson's ratio for the hydrogel. Further rearrangement of Eq. (6) removes the polymer volume fraction from the right-hand side of the formula and creates a modulus normalized by the degree of swelling on the left-hand side. By incorporating swelling effects with compressive modulus values, one is able to relate changes in this lumped parameter directly to changes in network structure

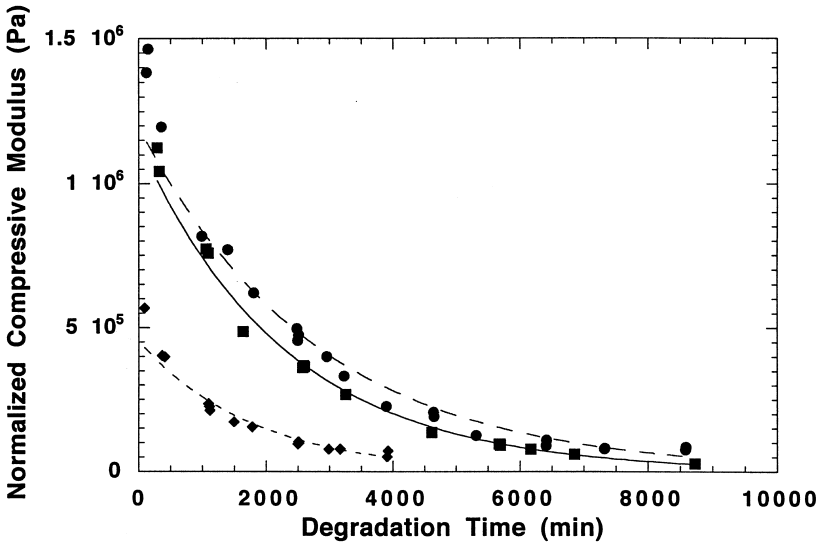

Fig. 6. Normalized compressive modulus behavior as a function of degradation time for hydrogels polymerized with varying macromer concentrations: (◆) 25 wt%; (■) 50 wt%; and (●) 70 wt%. The solid and dashed lines are exponential curves fit to the data points with time constants of $-0.00056\ \text{min}^{-1}$ (25 wt%), $-0.00043\ \text{min}^{-1}$ (50 wt%), and $-0.00036\ \text{min}^{-1}$ (70 wt%).

through their effect on $\bar{M}_C$.

$$K_{norm} = \frac{K}{(\nu_{2,S})^{1/3}} = \left(\frac{2(1+\nu)}{3(1-2\nu)}\right)\frac{\rho RT}{\bar{M}_C} \tag{7}$$

Applying the same methodology to the experimental data for the 50 wt% macromer sample in Fig. 4b yields the normalized modulus plot versus degradation time shown in Fig. 5. Compared to the true modulus, the normalization removes the additional decrease in modulus due to the increase in swelling with time (see Fig. 4a), leaving only the decrease due to the degradation of cross-links within the network. With each cross-link severed the average molecular weight between cross-links ($\bar{M}_C$) increases and the normalized compressive modulus (K_{norm}) decreases. Since the degree of swelling plotted in Fig. 4a is inversely related to the polymer volume fraction that appears in Eqs. (5) through (7), K and $\nu_{2,S}$ are both exponential functions with time, as shown by the data in Figs. 4a and b. The normalized modulus (K_{norm}), therefore, still decreases exponentially with degradation time, although at a slower rate than the un-normalized modulus. This behavior is shown by the exponential best-fit curve in Fig. 5. The normalized modulus data in Fig. 5 indicates that the $\bar{M}_C$ of this degrading hydrogel increases exponentially with time, since $\bar{M}_C$ is inversely related to the normalized modulus as shown in Eq. (7). Comparing the normalized modulus of all three samples in Fig. 6, the initial $\bar{M}_C$ and its exponential growth rate with time decrease with increasing macromer concentration.

Now that the factors affecting the mechanical strength of the hydrogels have been decoupled, the relationships between the macroscopic properties of these hydrogels and the degradation occurring within these networks can be examined more thoroughly. Since $\bar{M}_C$ and the cross-linking density are inversely proportional, cross-linking density is directly proportional to K_{norm} through Eq. (7). If the kinetics for the hydrolysis of the ester linkages are first order or pseudo first order with respect to the ester concentration, as discussed earlier, then the cross-linking density will decay exponentially with time. Using the proportionality given in Eq. (7), this exponential decay versus time can be extended to the normalized modulus. Through the best-fit exponential curves in Fig. 6, this relationship is shown to hold true for each of the degradation data sets at different macromer concentrations. Close examination of the initial $\bar{M}_C$ values of each run also reveals that $\bar{M}_C$ increases with the amount of solvent present during polymerization. This trend agrees with the earlier hypothesis of increased cyclization with solvent content. An increased amount of cyclization increases $\bar{M}_C$, causing samples of lower macromer concentration to swell to a greater extent. The increase in swelling causes these samples to have lower measured compressive modulus values, as shown in Fig. 4b, because Eq. (6) dictates that the compressive modulus is inversely proportional to the swelling ratio. Secondly, and perhaps more importantly, the increase in swelling and water concentration within the hydrogel accelerates the degradation kinetics given by Eq. (3). This causes the mechanical strength to decay more quickly (Figs. 4b and 6) and the swelling ratio to increase more rapidly (Fig. 4a) for degradation samples of lower macromer concentration.

3.3. Polymerization kinetics

As seen in Figs. 4–6, changes in the macromer concentration during polymerization dramatically alter the degradation behavior of the PEG-*b*-PLA hydrogels. The variety in both degradation kinetics and macroscopic properties of

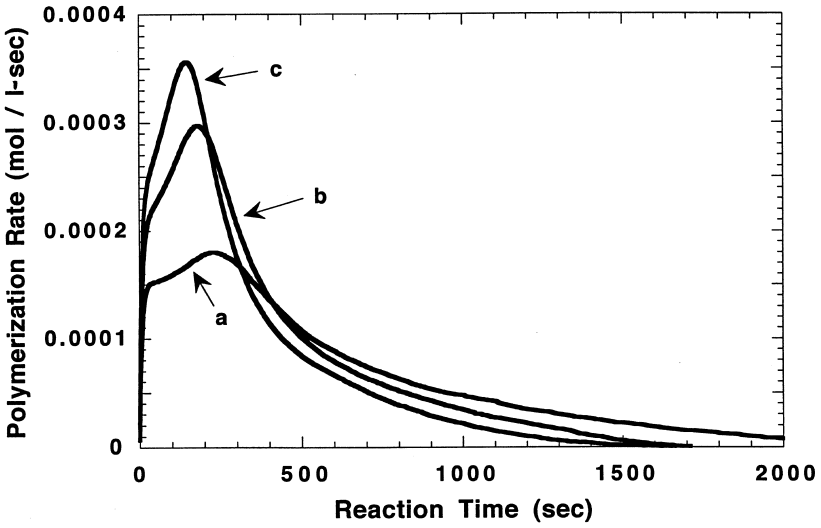

Fig. 7. Rate of polymerization as a function of time for solutions photopolymerized with three different 3400-5 macromer concentrations: (a) 50 wt%; (b) 66 wt%; (c) 71 wt%.

these gels during degradation has been primarily attributed to differences in network structure between the data sets. These differences have been inferred indirectly through theoretical calculations of $\bar{M}_C$. Another more direct method of quantifying differences in network structure is through the analysis of polymerization kinetics. Since network formation occurs during polymerization, any variation in the rate or degree of conversion between two otherwise similar samples can produce two networks with very different characteristics.

Fig. 7 shows the reaction behavior of the 3400-5 PEG-*b*-PLA macromer polymerized at various concentrations in solution. This figure presents the rate of polymerization (R_p) as a function of double bond conversion. Following an individual curve, one observes the onset of autoacceleration at a very early time. Autoacceleration occurs when the mobility of the terminating macromolecular radicals drops more quickly than the mobility of unreacted monomer in a cross-linked system, causing the rate of termination to drop and the polymerization rate to increase. This phenomena is commonly observed during the homopolymerization of smaller multifunctional monomers such as DEGDMA or PEG200DMA, which have higher cross-linking densities than the current PEG-*b*-PLA macromers [26]. Although the double bond concentration and resulting cross-linking density is lower in the PEG-*b*-PLA copolymer systems because of their high molecular weight backbones and presence of solvent, the mobilities of the terminating radicals in these swollen hydrogels are significantly restricted to cause an observable amount of autoacceleration.

After the maximum polymerization rate is reached for a given curve in Fig. 7, it is unclear whether autodeceleration occurs. During autodeceleration, the rate of propagation drops due to further mobility restrictions of the monomer species and propagating radicals. It has been observed that highly cross-linked polymers generally reach a limiting conversion well below 100% because their greatly reduced radical mobility limits further polymerization. The measured polymerization rate is reduced at higher conversions and longer times for each of the samples studied in Fig. 7. But the final conversion achieved for all of the systems is approximately 100% as confirmed by gel-fraction calculations and infrared measurements of acrylate double bond concentrations. Further kinetic studies are needed to ascertain the full details of what is occurring during these polymerizations and the degree to which radical mobility plays a role in determining polymerization kinetics.

The importance of the current analysis, however, is in comparison of the rate curve profiles of different macromer concentrations. As the macromer concentration in the polymerized solution is increased, the maximum rate of polymerization increases and is also shifted to earlier times. When the macromer concentration is lowered, the solvent concentration increases. The overall viscosity of the macromer solution is also visibly decreased. As mentioned previously, this environmental change increases the mobilities of all species within the polymerizing sample, including those of the terminating radicals. This increased mobility depresses the autoacceleration effect, resulting in a lower maximum rate at a later time, and a more constant rate curve overall.

The differences in the polymerization rate curves with macromer concentration translate into differences between the structures of their resulting hydrogel networks. The increase in cyclization with the amount of solvent present during polymerization has already been discussed. Another important factor is the length of the kinetic chains within the networks. The kinetic chain length (υ) is the number of times a propagating radical reacts with double bonds before terminating. If the pseudo-steady-state assumption is made for these polymerizations (rate of initiation (R_i) = rate of termination (R_t)) then υ is proportional to (R_p/R_i).

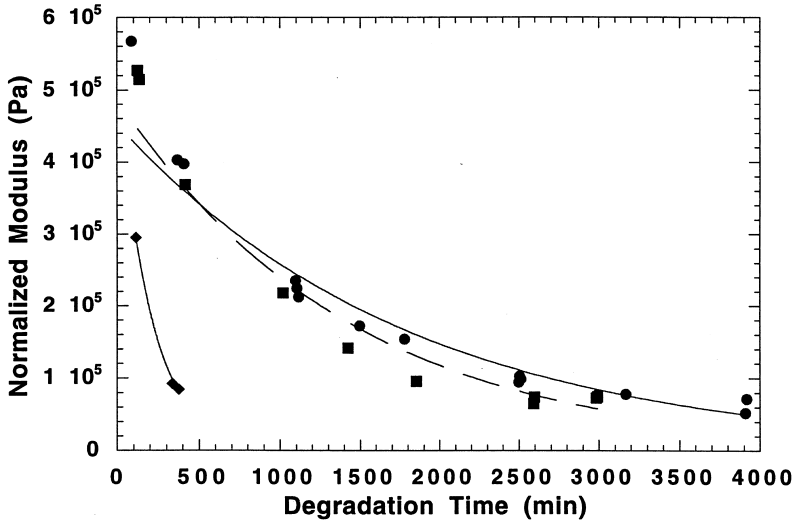

Fig. 8. Normalized modulus behavior with degradation time for three hydrogels polymerized from a 25 wt% 4600-5 macromer solution with varying monomer fractions of acrylic acid: (●) 0 mol%; (■) 25 mol%; and (◆) 95 mol%. The solid and dashed lines are exponential curves fit to the data points with time constants of $-0.00056\ min^{-1}$ (0 mol%), $-0.00071\ min^{-1}$ (25 mol%), and $-0.0049\ min^{-1}$ (95 mol%).

With the initiation rates being equal between the samples, the kinetic chain lengths formed within the networks during polymerization are directly proportional to the instantaneous propagation rates. Therefore, the 71 wt% solution with the sharp autoacceleration regime during polymerization will contain kinetic chains within its three-dimensional, cross-linked structure that are up to twice as long as the longest kinetic chains within the 50 wt% sample. The chemistry of the resulting cross-linked networks is the same, but their structures are certainly not.

Overall, the results drawn from the polymerization kinetic studies presented in Fig. 7 support the conclusion of earlier sections that the structure of the network within these novel hydrogel systems plays an important role in determining the degradation behavior of the network.

3.4. Acrylic acid effect

It has been shown that the degradation of these novel hydrogels is coupled to their network structure. To illustrate the importance of swelling behavior on their degradation, the same PEG-*b*-PLA macromer used earlier was copolymerized with acrylic acid. Compared to the large and bulky macromer, acrylic acid is a small and mobile monomer. Having only one double bond, acrylic acid cannot act as a cross-linking agent. It will, however, incorporate itself into the polymeric backbone of the hydrogel, altering the ratio of

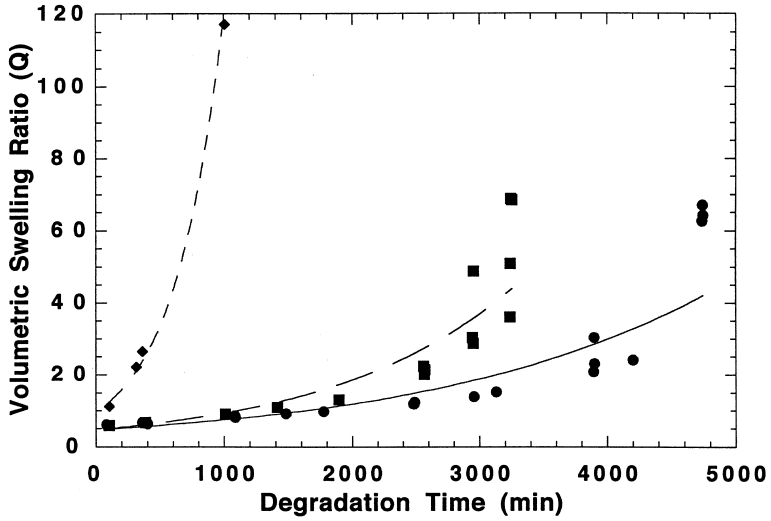

Fig. 9. Swelling behavior with degradation time for three hydrogels polymerized from a 25 wt% 4600-5 macromer solution with varying concentrations of acrylic acid: (●) 0 mol%; (■) 25 mol%; and (◆) 95 mol%. The solid and dashed lines are exponential curves fit to the data points with time constants of $0.00046\ min^{-1}$ (0 mol%), $0.00069\ min^{-1}$ (25 mol%), and $0.0025\ min^{-1}$ (95 mol%).

polyacrylate segments to PEG-*b*-PLA cross-links in the network.

Depending on the macromer being polymerized, the presence of acrylic acid segments along the polyacrylate chains may only slightly affect the average molecular weight between cross-links. With the 4600-5 macromer, for example, 95% of the network mass resides in the PEG-*b*-PLA segments. The increase in $\bar{M}_C$ could, however, be offset by the increased reactivity of the copolymer solution. For a given weight percent of the total monomer in solution, increasing the ratio of acrylic acid to high molecular weight PEG-*b*-PLA macromer will increase the concentration of the double bonds. As discussed earlier, increasing the double bond concentration (i.e. by decreasing the amount of water present) lowers the $\bar{M}_C$ of the final network by decreasing the chance of cycle formation during polymerization.

To understand which factor dominates in determining $\bar{M}_C$ for these systems, the normalized modulus values of three PEG-*b*-PLA hydrogels polymerized with various amounts of acrylic acid are plotted versus degradation time in Fig. 8. Here, it is shown that the fitted normalized modulus values (K_{norm}) at $t = 0$ increase with acrylic acid concentration. Using Eq. (7), this result indicates that the effect of lowering the degree of cyclization within the network dominates and that $\bar{M}_C$ decreases with an increasing acrylic acid fraction.

In Fig. 6 it was shown that the rate of degradation increased with $\bar{M}_C$. In Fig. 8, however, the rate of degradation of these hydrogels, measured by the rate of decay of the normalized modulus, increases with acrylic acid concentration. Examining the initial K_{norm} values, this means that the rate of degradation in these systems actually increases as the $\bar{M}_C$ values for the initial networks decrease. Therefore, another parameter must be controlling the degradation when acrylic acid is present.

Fig. 9 presents the swelling behavior during degradation of the same three data sets measured in Fig. 8. As the fraction of acrylic acid is increased, the degree of swelling increases. Similar to Fig. 4a, and in agreement with the microscopic degradation kinetics given by Eq. (4), the swelling ratios of all three curves increase exponentially with time. The absolute value of the swelling ratio as well as its exponential growth rate also increase with acrylic acid fraction. By the time the acrylic acid content is 95 mol%, the total degradation time is approximately one-fifth that of the hydrogel formed from the pure PEG-*b*-PLA macromer and the growth rate of the swelling is approximately five times as large.

Acrylic acid, as its name suggests, is acidic in nature with a p*K*a of 4.25. In the phosphate-buffered saline solution at a controlled pH of 7.4, a majority of the acrylic acid segments polymerized into the hydrogel will therefore de-protonate, leaving fixed, negatively charged species attached to the network. The negative charges will attract additional water molecules into the polymer network, increasing the degree of swelling within the samples and, through the kinetic reaction of Eq. (3), increasing the rate of degradation of the hydrogels as well. The increased swelling of samples copolymerized with acrylic acid influences the degradation kinetics to such a degree that, even with smaller measured $\bar{M}_C$ values, they degrade more rapidly than the pure PEG-*b*-PLA macromer polymerized under the same conditions.

4. Conclusions

The degradation behavior of these cross-linked hydrogel networks is much different from degradable, linear systems such as PLA and PGA. For hydrogels of the same polymer chemistry, network topology, measured by such parameters as $\bar{M}_C$, strongly influences the degradation behavior. The results demonstrate the strong coupling of network microstructure to the degradation rate, swelling ratio, and mechanical strength of the PEG-*b*-PLA hydrogels. The network structure is formed during polymerization and can, therefore, be altered by changing the polymerization conditions. Photopolymerizations offer facile control of light intensity, initiator concentration, and exposure time, as well as to macromer concentration and solution temperature. Increasing the macromer concentration in the polymerizing solutions leads to networks with lower characteristic $\bar{M}_C$ values (higher cross-linking densities) and hydrogels with increased mechanical strength, lower swelling ratios, and lower degradation rates.

As expected, the chemistry of the polymer also plays an important role in determining the macroscopic properties of the PEG-*b*-PLA hydrogels. Copolymerization of the PEG-*b*-PLA macromer with acrylic acid leads to stronger gels with higher swelling ratios and degradation rates. This unique combination of properties is attributed to the partially ionized character of the poly(acrylic acid) repeat unit in the 7.4 pH degradation environment.

Overall, tailoring the network structure of a degradable hydrogel by altering its polymerization conditions allows optimization of macroscopic properties and degradation behavior. The ability to adjust structural parameters in addition to chemistry should make this class of cross-linked materials more attractive for a number of specific biomedical applications.

Acknowledgements

The authors thank the National Science Foundation and the Rubber Division of the American Chemical Society for support of this work through fellowships to ATM as well as a grant from the National Institutes of Health (DE12998). The technical assistance of Michael Wu and Kathryn Riddle in obtaining portions of the experimental data is also very much appreciated.

References

[1] Langer R. Science 1990;249(4976):1527–33.
[2] Smith CR, Gaterud MT, Jamiolkowski DD, et al. US Patent, 4,741, 1998, 337.
[3] Tamada J, Langer R. J Biomater Sci 1992;3(4):315–53.
[4] Merrill EW, Dennison KA, Sung C. Biomaterials 1993;14(15):1117–26.
[5] Peppas NA. Applications. Hydrogels in medicine and pharmacy, 2. Boca Raton, FL: CRC Press, 1986.
[6] Graham NB, McNeill ME. Makromol Chem Macrmol Symp 1988;19:255–73.
[7] Zhu KJ, Lin XZ, Yang SL. J Appl Polym Sci 1990;39(1):1–9.
[8] Li SM, Rashkov I, Espartero JL, Manolova N, Vert M. Macromolecules 1996;29(1):57–62.
[9] Sawhney AS, Chandrashekhar PP, Hubbell JA. Macromolecules 1993;26(4):581–7.
[10] West JL, Hubbell JA. Reactive Polym 1995;25(2–3):139–47.
[11] Hill-West JL, Chowdhury SM, Sawhney AS, Pathak CP, Dunn RC, Hubbell JA. Obstet Gynecol 1994;83(1):59–64.
[12] Hill-West JL, Chowdhury SM, Slepian MJ, Hubbell JA. Proc Natl Acad Sci USA 1994;91(13):5967–71.
[13] Elisseeff J, Anseth K, Sims D, et al. Proc Natl Acad Sci USA 1999;96(6):3104–7.
[14] Iza M, Stoianovici G, Viora L, Grossiord JL, Couarraze G. J Controlled Release 1998;52(1–2):41–51.
[15] Peppas NA. Fundamentals. Hydrogels in medicine and pharmacy, 1. Boca Raton, FL: CRC Press, 1986.
[16] Gopferich A. Macromolecules 1997;30(9):2598–604.
[17] Burkersroda F, Gref R, Gopferich A. Biomaterials 1997;18(24):1599–607.
[18] Siparsky GL. The degradation of poly(lactic acid) and its copolymers with poly(e-caprolactone): hydrolysis and permeability, MS thesis, Colorado School of Mines, CO, 1995.
[19] Tamada JA, Langer R. Proc Natl Acad Sci USA 1993;90(2):552–6.
[20] Kenley RA, Lee MO, Mahoney TR, Sanders LM. Macromolecules 1987;20(10):2398–403.
[21] Bezzi S, Riccoboni L, Sullam C. Dehydration products of lactic acid typifying the transformation of cyclic esters into linear esters, Italian Academy of Science, 1936.
[22] Gopferich A, Langer R. Macromolecules 1993;26(16):4105–12.
[23] Elliott JE, Anseth J, Bowman CN. Submitted for publication.
[24] Flory PJ. Principles of polymer chemistry, Ithaca, NY: Cornell University Press, 1953. chap. 13.
[25] Anseth KA, Bowman CN, Brannon-Peppas L. Biomaterials 1996;17(17):1647–57.
[26] Anseth KA, Kline LM, Walker TA, Anderson KJ, Bowman CN. Macromolecules 1995;28(7):2491–9.